Directed percolation describes lifetime and growth of turbulent puffs and slugs

Maksim Sipos and Nigel Goldenfeld

Department of Physics, Loomis Laboratory of Physics, University of Illinois at Urbana-Champaign, 1110 West Green Street, Urbana, Illinois 61801-3080, USA

We show that directed percolation (DP) simulations in a pipe geometry in $3+1$ dimensions capture the observed complex phenomenology of the transition to turbulence. At low Reynolds numbers (Re), turbulent puffs form and spontaneously relaminarize. At high Re, turbulent slugs expand uniformly into the laminar regions. In a spatiotemporally intermittent state between these two regimes of Re, puffs split and turbulent regions exhibit laminar patches. DP also captures some of the quantitative features of the transition, with a superexponentially diverging characteristic lifetime below the transition. Above the percolation threshold, active (turbulent) clusters expand into the inactive (laminar) phase with a well-defined velocity whose scaling with control parameter (Reynolds number or percolation probability) is consistent with experimental results. Our results provide strong evidence in favor of a conjecture of Pomeau.

The transition from laminar to turbulent flow, studied first by Reynolds [1] in pipes, remains a source of complex and fascinating phenomenology. Varying the dimensionless parameter bearing his name, $\mathrm{Re} \equiv UL/\nu$, where U and L are characteristic flow velocity and length scales and ν is the kinematic viscosity, Reynolds observed localized clusters of turbulence, now commonly called "puffs," that can spontaneously split or decay. Later, Wygnanski and Champagne [2] systematically described the phase diagram of the laminar to turbulent transition as a function of the Reynolds number, and the dynamics of the transition is an active area of investigation today [3–5]. Laminar pipe flow is known to be linearly stable for all Reynolds numbers, but small disturbances can trigger a transition to the turbulent state [6]. For sufficiently low Re the fluid flow is always laminar and any turbulent disturbances decay immediately. However, when $1650 < \mathrm{Re} < 2050$, turbulent puffs are metastable and their lifetime grows superexponentially with Re [7]. For larger values of Re, the characteristic lifetime of these puffs grows, and they begin to split and show complex spatiotemporal behavior [8,9]. The splitting process continues, until Re exceeds a critical value $\mathrm{Re}_c \sim 2500$, above which and for a sufficiently large inlet disturbance, a uniform state of turbulence, a "slug," grows with a clearly defined turbulent-laminar interface and a velocity that scales approximately with $\sqrt{\mathrm{Re} - \mathrm{Re}_c}$ [10,11]. The phase diagram of pipe flow turbulence is shown schematically in Fig. 1. The purpose of this Rapid Communication is to show in detail that the phenomenology and quantitative details of many features of the laminar-turbulent transition are consistent with the nonequilibrium phase transition in the universality class of directed percolation (DP), as originally conjectured by Pomeau [12] and continued in subsequent works by many authors (see, e.g., [13] and references therein). Our work measures the lifetime of active states in DP in a pipe geometry, finding agreement with the superexponential functional dependence recently measured by Hof *et al.* [7]. We also measure the growth rate of active DP clusters in the supercritical directed percolation and show that our scaling results are in good agreement with available experimental data on the growth rate of turbulent slugs [10]. These results show that dynamical phase transition phenomena may be described by directed percolation, supporting

earlier detailed observations of the DP critical exponents in a fluctuating turbulent liquid crystal system driven by external forcing [14,15].

The analogy between DP and the turbulent-to-laminar transition is the following: Active states in a three-dimensional lattice correspond to coarse-grained regions of size $\sim\eta$ where the turbulence intensity exceeds a threshold (here η is the viscous scale), whereas inactive states correspond to patches of the fluid which are laminar. The dimension along the percolating direction is associated with time t in the usual interpretation of DP as a dynamical process. The percolating probability p is analogous to the Reynolds number Re in the vicinity of the percolation transition, but the mapping need not be linear. For the metastable puffs, $\mathrm{Re} < 2050$ region is mapped to $p < p_c$ whereas for the growing fronts, $\mathrm{Re} > 2500$ is mapped to $p > p_c$. The critical region maps into the spatiotemporal regime, as summarized in Fig. 1, but this region and p_c are not strictly defined except in the limit of infinite system size.

We simulate DP in $3+1$ dimensions, in the reference frame of the traveling puff, which usually travels more slowly than the laminar mean flow velocity U. Here we use the bond percolation process. The inlet disturbance in pipe flow experiments is modeled as the initial region of active (turbulent) sites. At each time step, each turbulent site will stay turbulent with probability p, or decay to the laminar state with probability $1 - p$. With probability p, the turbulent lattice site (x,y,z) can also activate (infect) adjacent laminar sites. Because the bond percolation process occurs on a diagonal lattice, the adjacent sites are chosen differently for odd and even time steps. For even time steps, adjacent sites are $(x + 1,y,z)$, $(x,y + 1,z)$, and $(x,y,z + 1)$. For odd time steps, adjacent sites are $(x - 1,y,z)$, $(x,y - 1,z)$, and $(x,y,z - 1)$. All updates are performed sequentially.

Lifetime of turbulent puffs. The survival probability of turbulent puffs in pipe flow is known to be memoryless [16,17],

$$P(\mathrm{Re},t) = \exp\left(-\frac{t - t_0}{\tau(\mathrm{Re})}\right), \qquad (1)$$

where $t > t_0$. Here, the survival probability $P(\mathrm{Re},t)$ refers to the probability that the turbulent puff still exists after flowing
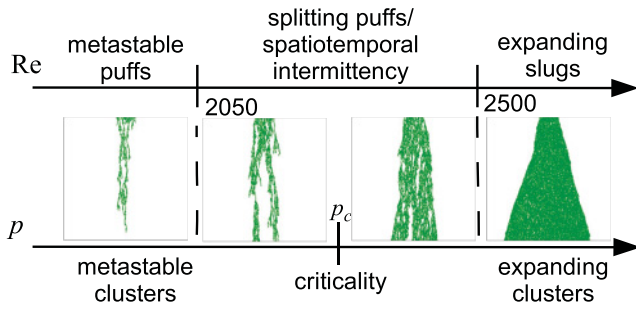
FIG. 1. (Color online) Comparison of the phenomenology of transitional turbulence as a function of Re with that of DP in $3 + 1$ dimensions as a function of p, both in a pipe geometry.

for time t, t_0 is the formation time of the puff, and $\tau(\mathrm{Re})$ is the characteristic lifetime. In Hof *et al.*'s work t_0 was a constant ($70D/U$ where U is the mean flow velocity and D is the pipe diameter) [7]. By measuring $P(\mathrm{Re},t)$ for specific times t and Reynolds numbers Re, Hof *et al.* calculated $\tau(\mathrm{Re})$ from (1). They discovered that τ scales superexponentially with Reynolds number [7], fitting well a parametrization of the form

$$\tau(\mathrm{Re}) = \tau_0 \exp[\exp(c_1\mathrm{Re} + c_2)], \quad (2)$$

where $\tau_0 \sim D/U$.

The survival probability $P(p,t)$ in our DP measurements is the probability that there will be active sites left in the lattice after t DP steps. From $P(p,t)$, the lifetime of the disturbance τ can be measured just as it was by Hof *et al.* This idea is illustrated in the snapshots of the simulation in Fig. 2(a). Here, DP is simulated in $3 + 1$ dimensions in a pipe of radius of five lattice sites. In this simulation p is less than p_c, and so the puff eventually decays. Generally, one can measure the lifetime with a three-dimensional lattice where two of the spatial dimensions span a disk of radius of R lattice points (corresponding to the pipe radius), with fixed boundary conditions. However, the measurement of lifetime in this way over many orders of magnitude is made difficult because of the system size. The lifetime measurements must be repeated many times to be able to obtain sufficient statistics. However, when p is close to the critical percolation threshold p_c, the correlation length $\xi_\perp \sim (p - p_c)^{\nu_\perp}$ along a space dimension becomes larger than R, and the nominally $(3 + 1)$-dimensional DP is effectively $(1 + 1)$-dimensional. Thus, to get sufficient statistics we simulate DP in a one-dimensional lattice of length N that is initially made to be active in a subregion of length N_0. Below the DP critical point the active states will eventually decay into the absorbing state. In a finite-sized system, the decay can always occur, but we find that the characteristic lifetime τ of the decay grows superexponentially with percolation threshold p, and beyond a certain percolation probability, the average lifetime of the active state is too large to be measurable on a computer.

Hof *et al.* were able to calculate τ via (1) by measuring $P(\mathrm{Re},t)$. Even though they could only extend t to $3450D/U$, they were able to resolve P to 100 ppm, giving them effective measurements of τ over eight orders of magnitude. In the case of directed percolation, one cannot use this procedure, since t_0 is not constant, but instead depends on the percolation
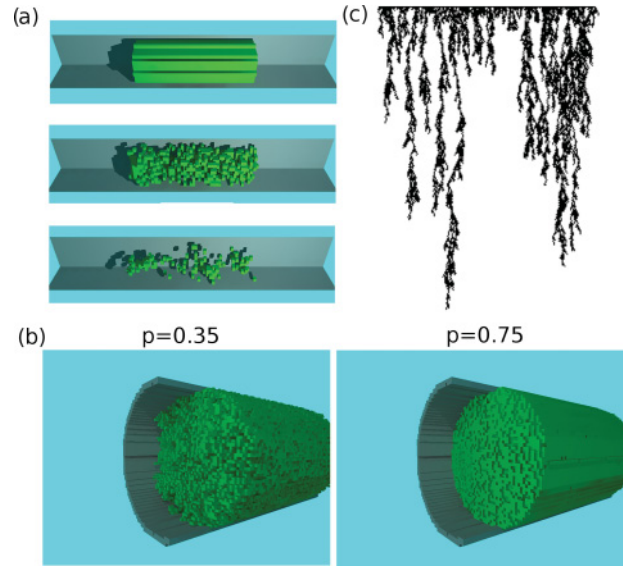

FIG. 2. (Color online) (a) Illustration of the decay of an active cluster in subcritical directed percolation in $3 + 1$ dimensions in pipe geometry. In this figure the length of the pipe extends horizontally, and the active sites in percolation are displayed with green cubes. Inactive sites are not shown. (b) Different front shapes in the growing front bond DP model. Rough fronts occur for small $p - p_c$ whereas smoother fronts occur for large $p - p_c$. (c) Time evolution of an initially active 180 contiguous sites percolating downward simulated via bond percolation for $p = 0.61 < p_c$. The active state (in black) fully decays into the absorbing state (white) after about 250 steps.

probability p. In directed percolation, t_0 is the time over which the initial state is remembered by the system. Hence, for each value p we must measure the survival lifetimes of many instantiations of directed percolation. The cumulative distribution function (CDF) of these survival lifetimes then approximates the survival probability $P(p,t)$, as long as sufficiently many instantiations have been performed. From the fit of the form (1) to the CDF data, one can read off $\tau(p)$ and $t_0(p)$. Our measurements of $\tau(p)$ for a lattice of size $N = 100$ and $N_0 = 20$ are given in Fig. 3(a). The line in the figure is obtained by fitting τ to (2). The inset shows the linear fit to $\log \log \tau(p)/\tau_0$. Sufficiently far away from the critical point p_c, we find that the linear fit deviates, indicating that the superexponential behavior may somehow be related to the diverging correlation lengths at the critical point.

From the CDF data, we can evaluate the survival probability functions analogously to Fig. 2 of [7]. Figure 3(b) shows our numerical data $P(p,t)$ for four different times (S curves), along with the model $P(p,t) = \exp[-(t - t_0)/\tau(p)]$. To evaluate the model fit, we use the value of $t_0(p_{0.2})$ where $p_{0.2}$ is found by setting $P(p_{0.2},t) = 0.2$. Note that the fact that the S curves become steeper with p is a characteristic of the superexponential scaling of $\tau(p)$.

The numerical data presented so far in the paper has been measured in a finite volume of size $N = 100$. Finite size effects in DP have been investigated thoroughly in the literature [18]. We ran our simulations in a volume bound only by the range of the integers on our computer (0 to $2^{63} - 1$), and we did not find any qualitative differences regarding the superexponential scaling of $\tau(p)$.
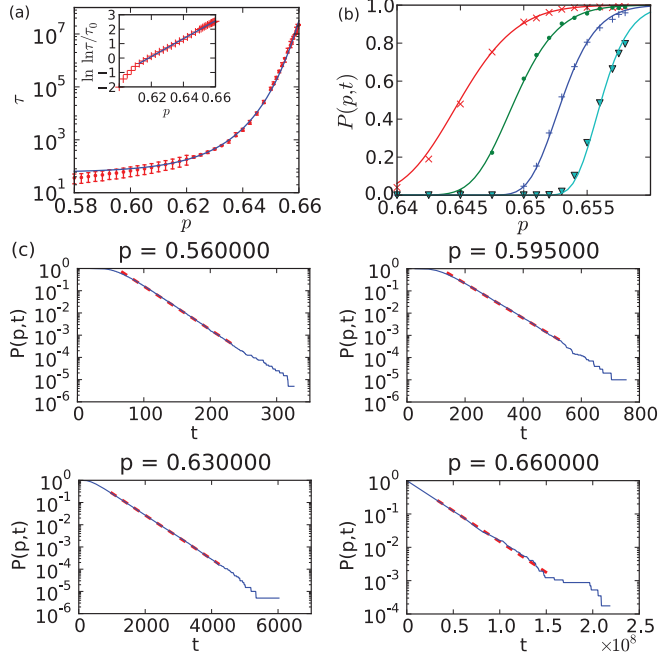
FIG. 3. (Color online) (a) Superexponential scaling of the characteristic lifetime τ. The line indicates the fit to (2). Error bars indicate 95% confidence intervals from a Kolmogorov-Smirnov test (for $p > 0.62$) and 90% confidence intervals from a χ^2 test (for $p \leqslant 0.62$). In the inset, $\tau_0 = 0.017$. (b) Numerical data for survival probabilities $P(p,t)$ (points) and a fit to (1) with τ given by (2) (solid lines). Data shown for $t = 300$ (red crosses), 1000 (green dots), 6000 (blue pluses) and 80 000 (cyan triangles). The value of p_c observed corresponds to that of $(1 + 1)$-dimensional bond percolation. (c) Measured survival probabilities as functions of t for four different values of percolation probability p. Blue solid line indicates measured data, whereas red dashed line indicates a fit to the exponential distribution. Deviations from exponential distribution for small t are due to nonzero t_0.

Growth rate model. When $p > p_c$ active DP clusters grow in the pipe. We measured their growth rate and related it to the growth rate of turbulent slugs. The speed at which the front of the percolating clusters propagate into the neighboring inactive region is given by $G \sim \xi_\perp/\xi_\parallel \sim (p - p_c)^{\nu_\parallel - \nu_\perp}$, where $\xi \sim (p - p_c)^{-\nu}$ is the correlation length in the direction of space (denoted by $\perp$) or in the direction of time (denoted by $\parallel$). Using the above prescription and numerical values of DP critical exponents [18], one should expect that $G \sim (p - p_c)^\gamma$ where $\gamma = 0.524$ in $(3 + 1)$-dimensional DP, whereas $\gamma = 0.637$ in $1 + 1$ dimensions. These power laws are close to the exponent 0.5 first proposed in 1986 [10], as well as in modern experiments [11]. However, the data are not sufficient yet to differentiate between two such close power law exponents.

Measurements of the growth rate G of an initially active region in $3 + 1$ DP in a pipe geometry are shown in Fig. 4. The measurements were made by simulating bond DP with $p > p_c$ and measuring the positions of the two fronts as functions of time. During the numerical simulation we also measure the correlation length $\xi_\perp$ by calculating the root-mean-square height (i.e., roughness) of the turbulent-laminar interface. The agreement with theoretical expectation is good, and we see
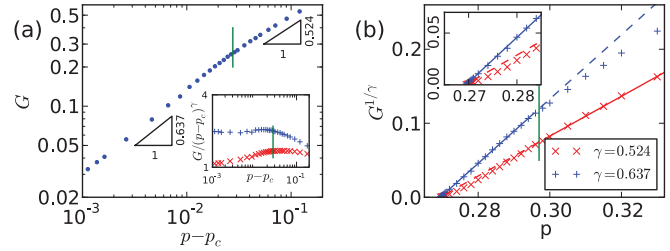

FIG. 4. (Color online) Measured values of front propagation velocity G (red crosses) compared to theoretical prediction for $(3 + 1)$-dimensional and $(1 + 1)$-dimensional DP. Green vertical line indicates the value of p for which $\xi_\perp$ exceeds $1.2R$. We call this value p_R. (a) Plot indicating the power law crossover of $G(p)$. Inset shows that $G/(p - p_c)^{0.637}$ is roughly constant for $p < p_R$ and similarly $G/(p - p_c)^{0.524}$ for $p > p_R$. (b) Both regimes of DP have the same critical point p_c (within the error of our measurements). The linear fits to $G^{1/\gamma}$ are shown in solid lines. Extrapolations are indicated with dashed lines, and they cross at the same p_c. This value of p_c corresponds to that of $(3 + 1)$-dimensional bond percolation.

numerical evidence for the crossover from $3 + 1$ to $1 + 1$ dimensions. When $p - p_c \ll 1$, then $\xi_\perp > R$ and the system is effectively $1 + 1$ dimensional. In Fig. 4(b), we have plotted $G^{1/\gamma}$ versus p for different choices of γ corresponding to $(1 + 1)$- and $(3 + 1)$-dimensional DP. We see clearly the crossover between the expected regimes [19]. Note that in this plot we did not need to guess p_c: both scaling regimes yield the same p_c. It is difficult however to extend the data for $G(p)$ close to p_c. Due to the finite size of the system, when $p - p_c$ is small, the active regions split and may decay into the absorbing state. This makes it difficult to clearly measure front propagation velocity. On the other hand, when $p - p_c$ is large, the scaling breaks down. Thus we expect the power law exponent of 0.524 to be observable only in an intermediate regime of $p - p_c$, sufficiently close to p_c but still such that $\xi < R$.

One other aspect of the phenomenology of pipe flow is captured by the DP model, namely, that the fronts of active regions with $p - p_c \ll 1$ are much rougher than when $p - p_c$ is large. This is because the density of active states within the region is an increasing function of p. Furthermore, the width of the front is related to the spatial correlation length $\xi_\perp$ which becomes small when $p - p_c$ is large. The difference between the rough and smooth front regimes is shown in Fig. 2(b). This is analogous to the results in pipe flow experiments using hot wire measurements, where puff structures were found to have rough edges whereas slugs have clearly defined fronts [2,20].

Conclusion. The DP simulations of characteristic lifetime presented in this paper have been performed via the bond percolation algorithm. However, we found superexponential scaling of $\tau(p)$ for site percolation too. Therefore, the superexponential scaling of the lifetime is likely a universal characteristic of the directed percolation process. Goldenfeld *et al.* proposed that this superexponential character of the turbulent puff lifetime can be described by extreme value statistics [21], because puff decay occurs when turbulent energy fails to attain the required threshold at all points in the puff [22]. In the usual central limit theorem, under

appropriate conditions [23] the distribution of a sum of N random variables tends to a Gaussian distribution for large N. However, a maximum (or minimum) of N random variables is instead superexponentially distributed with three universality classes [21], selected by the underlying probability distribution of $\{x_i\}$. In Fig. 2(c) we show a time evolution of an initially active cluster percolating with $p < p_c$. The lifetime of the entire cluster is the lifetime of the longest active "strand" percolating downward. Assuming that strand lifetimes are independent and identically (exponentially) distributed, then the lifetime of the longest strand is given by the type I Fisher-Tippett distribution $\exp[-\exp(-p)]$. This argument has also been used to explain the superexponential distribution of size of the largest connected cluster in ordinary (isotropic) percolation [24], and it was found there that correlations between cluster sizes (analogous to strand lifetimes) do not influence the superexponential scaling.

The DP model we proposed in this paper can account for the superexponential lifetime of the turbulent puffs, as well as the uniform growth rate of turbulent slugs. As shown in Fig. 1, the transition between these two regimes ($2050 < \mathrm{Re} < 2500$) occurs through the splitting and interactions of puffs. The spatiotemporal patterns of coarse-grained turbulent intensity obtained from a direct numerical simulation [9] bear similarities to those of directed percolation, but the data are not adequate to make a quantitative analysis. Recently, we learned of work by Barkley, which uses a coupled map and a shear field to model the laminar-turbulent transition [25]. It is possible that this model is in the DP universality class also.

[1] O. Reynolds, Philos. Trans. R. Soc., Ser. A **174**, 935 (1883).

[2] I. Wygnanski and F. H. Champagne, J. Fluid Mech. **59**, 281 (1973).

[3] R. Kerswell, Nonlinearity **18**, R17 (2005).

[4] B. Eckhardt, T. M. Schneider, B. Hof, and J. Westerweel, Annu. Rev. Fluid Mech. **39**, 447 (2007).

[5] B. Eckhardt, Philos. Trans. R. Soc., Ser. A **367**, 449 (2009).

[6] H. Salwen, F. Cotton, and C. Grosch, J. Fluid Mech. **98**, 273 (1980), ISSN 0022-1120.

[7] B. Hof, A. de Lozar, D. J. Kuik, and J. Westerweel, Phys. Rev. Lett. **101**, 214501 (2008).

[8] D. Moxey and D. Barkley, Proc. Natl. Acad. Sci. USA **107**, 8091 (2010).

[9] B. Hof, M. Avila, A. de Lozar and K. Avila (unpublished).

[10] K. Sreenivasan and R. Ramshankar, Physica D **23**, 246 (1986).

[11] A. de Lozar and B. Hof, e-print arXiv:1001.2481.

[12] Y. Pomeau, Physica D **23**, 3 (1986).

[13] P. Manneville, Phys. Rev. E **79**, 025301(R) (2009).

[14] K. A. Takeuchi, M. Kuroda, H. Chate, and M. Sano, Phys. Rev. Lett. **99**, 234503 (2007).

[15] K. A. Takeuchi, M. Kuroda, H. Chate, and M. Sano, Phys. Rev. E **80**, 051116 (2009).

[16] A. P. Willis and R. R. Kerswell, Phys. Rev. Lett. **98**, 014501 (2007).

[17] H. Faisst and B. Eckhardt, J. Fluid Mech. **504**, 343 (2004).

[18] H. H. Hinrichsen, Adv. Phys. **49**, 815 (2000).

[19] See Supplemental Material at http://link.aps.org/supplemental/10.1103/PhysRevE.84.035304 for the crossover in density of sites in the slug.

[20] M. Nishi, Bülent Ünsal, F. Durst, and G. Biswas, J. Fluid Mech. **614**, 425 (2008).

[21] R. A. Fisher and L. H. C. Tippett, Proc. Cambridge Philos. Soc. **24**, 180 (1928).

[22] N. Goldenfeld, N. Guttenberg, and G. Gioia, Phys. Rev. E **81**, 035304 (2010).

[23] W. Feller, *An Introduction to Probability Theory and Its Applications* (John Wiley and Sons, New York, 1968).

[24] M. Z. Bazant, Phys. Rev. E **62**, 1660 (2000).

[25] D. Barkley, Phys. Rev. E **84**, 016309 (2011).